

STIMULATED RAMAN SCATTERING BY AN INTENSE  
RELATIVISTIC ELECTRON BEAM SUBJECTED  
TO A RIPPLED ELECTRIC FIELD

by

G. Bekefi and R. E. Shefer

Preprint PFC/JA-79-1  
Plasma-Research Report

PRR 79/3  
February 1979

STIMULATED RAMAN SCATTERING BY AN INTENSE RELATIVISTIC  
ELECTRON BEAM SUBJECTED TO A RIPPLED ELECTRIC FIELD\*

G. Bekefi and R. E. Shefer

Department of Physics and Research Laboratory of Electronics  
Massachusetts Institute of Technology  
Cambridge, Massachusetts 02139

ABSTRACT

Generation of submillimeter radiation by stimulated Raman scattering in an intense relativistic electron beam subjected to a spatially periodic transverse electric field is examined. The requisite electric field modulation can be obtained by rippling the wall of the conducting drift tube. When the electron beam is subjected to a periodic longitudinal electric field, short wavelength plasmons, rather than photons are generated. The growth rate and other parameters related to this instability are discussed.

\*This work was supported by the National Science Foundation (Grant ENG77-00340-A01) and the United State Air Force Office of Scientific Research (Grant AFOSR77-3143B).

## I. INTRODUCTION

Free electron lasers based on stimulated Compton<sup>1,2</sup> or Raman<sup>3,4,5</sup> scattering by relativistic electron beams require a low frequency pump wave for their operation. To date, consideration has been given to pump waves that are either of the form of a static, spatially periodic magnetic field<sup>1,2,4,5</sup> <sup>or</sup> a propagating electromagnetic wave.<sup>3</sup> In order to achieve interesting levels of submillimeter radiation, one must strive for the largest pump amplitudes (at the shortest wavelengths) that are technically feasible. When one contemplates using an electromagnetic pump, a microwave generator capable of delivering 400 to 1000MW of power at a wavelength of several centimeters is needed. When the pump is in the form of a static, periodic transverse magnetic field of amplitude  $B_{o\perp}$  and spatial periodicity  $\ell$ , values of the ratio  $B_{o\perp}/\ell \leq 800\text{G/cm}$  with  $0.6 < \ell < 3.2\text{cm}$  have been achieved so far; however, larger modulations would be most desirable.

Here we explore the possibility of using a quasi-static electric field as the pump. In contrast to the aforementioned techniques, the electric field pump exploits the intense space charge fields of an unneutralized electron beam itself and is self-generated, thus avoiding the difficulties of manufacturing strong pumps having the desired short wavelength periodicity. Intense space-charge fields are associated with beams of large current density and we shall therefore concern ourselves only with pulsed, relativistic electron beams carrying currents that are typically 10kA and greater. Here also stimulated Raman<sup>6,7,8</sup> scattering, (requiring dense plasmas with Debye lengths that are short compared with relevant wavelengths) takes precedence over Compton<sup>8,9,10,11</sup>

scattering, (where the Debye length is comparable with the wavelength), and it is the former process that will be of interest to us.

Two kinds of electric field pump may be of interest. In the one, the electric field is polarized transverse to the direction of beam propagation, and in the other it is polarized parallel to it. These cases are illustrated in Fig. 1. When the modulation is transverse, the three-wave parametric process is of the stimulated Raman type leading to the generation of short wavelength photons. When the modulation is parallel to the beam, all three participating waves are longitudinal waves resulting in the emission of short wavelength plasmons. The two situations will be treated separately. We begin with the problem of transverse modulation.

## II. THE TRANSVERSE ELECTRIC PUMP

In the upper part of Fig. 1, the electric field is shown to be oriented perpendicular to the direction of beam propagation. In the rest frame of the moving electrons, this pump appears as a transverse electromagnetic wave traveling antiparallel to the beam. It induces, via the ponderomotive force (i.e. radiation pressure) unstable axial density fluctuations which, in turn, give rise to growing backward and forward scattered transverse electromagnetic waves. The backscattered wave (propagating parallel to the beam direction) is doubly Doppler upshifted in frequency and represents the source of submillimeter radiation (photons). The frequency of the backscattered wave, its growth rate and other relevant data are summarized in the upper part of Table I. Indeed, these results

are the same as those derived<sup>7</sup> for Raman scattering for a static, periodic magnetic field pump, with the understanding that the magnetic modulation amplitude  $B_{O\perp}$  for a magnetic pump plays the same role as  $E_{O\perp}$  plays in the electric field pump. Thus, for example, a magnetic pump with a typical amplitude  $B_{O\perp} = 0.04\text{T}(400\text{G})$  acting on a given electron beam yields the same stimulated Raman growth rate as an electric pump of amplitude  $E_{O\perp} = cB_{O\perp} \approx 120\text{kV/cm}$ .

An electron beam of radius  $a$ , uniform velocity  $v$  and current density  $J$  has associated with it a radial space charge electric field given by  $J r/2\epsilon_0 v$  where  $r$  is the radius vector. At the beam edge  $r=a$ , the electric field is  $J a/2\epsilon_0 v$ , which for a relativistic beam ( $v \approx c$ ) of radius  $0.5\text{cm}$  and carrying a current of  $20\text{kA}$  gives a field of  $\sim 2.4 \times 10^6 \text{V/cm}$ . Thus, a 10 percent spatial field modulation appropriately induced leads to a pump of about the desired strength. One way to achieve this modulation is to ripple the wall of the conducting drift tube as illustrated in Fig. 2. It will be shown momentarily that the potential  $V(r)$  at any point  $r$  within the beam is a function of both the beam radius  $a$  and the proximity of the conducting wall, that is, the distance  $b$ . On account of this radial potential distribution the beam electrons acquire a radial distribution of axial velocities. At a given radius, the rippling of the wall induces an axial rippling in the particle velocities. Since the current density is constant, this in turn causes a rippling in the space charge density and thus in the radial electric field.

We compute the radial electric field  $E_{\perp}(r=a)$  at the beam edge in an approximate way by assuming that the potential  $V$  is a function only of radius  $r$ . The neglect of any  $z$  (i.e. axial) depen-

dence, as if each section of the rippled drift tube were infinitely long, is not too serious provided that the modulation depth is small compared with the periodicity. More specifically, we assume that  $(b_2 - b_1)^2 \ll \ell^2$  (see Fig. 2). (That squared quantities rather than linear dimensions enter the inequality comes from Poisson's equation  $\nabla^2 V = -\rho/\epsilon_0$ .)

Consider, then, an infinitely long drift tube of radius  $b$  containing an electron beam of radius  $a$  and uniform current density  $J$ . The beam is subjected to an axial magnetic field  $B_z$  so strong that (a) all electron motions can be considered purely axial, and (b) the beam azimuthal self-magnetic field can be neglected compared with  $B_z$ . For convenience, the potential at the center of the beam ( $r=0$ ) is taken to the zero and the potential of the cylindrical drift tube is maintained at  $V_b$  (and equals the anode potential). The potential difference between the source of the electrons (i.e. the cathode situated at a large distance  $z$  from the region under consideration), and the drift tube is denoted by  $V_0$ .

The problem is an electrostatic one requiring a solution of Poisson's equation

$$\begin{aligned} \frac{1}{r} \frac{\partial}{\partial r} \left( r \frac{\partial V}{\partial r} \right) &= \frac{J}{\epsilon_0 v(r)} & r \leq a \\ &= 0 & a \leq r \leq b \end{aligned} \quad (1)$$

subject to the energy conservation equation,

$$\begin{aligned} m_0 c^2 [\gamma(r) - 1] &= e [V_0 - V_b + V(r)] \\ \gamma(r) &= [1 - (v(r)/c)^2]^{-1/2} \end{aligned} \quad (2)$$

and the boundary condition,

$$a \ln \left( \frac{b}{a} \right) \left[ \frac{\partial V}{\partial r} \right]_{r=a} = V_b - V_a \quad (3)$$

The last equation is a statement of the fact that the potential is continuous across the beam-vacuum interface  $r=a$  where it has a value  $V_a$ ; it has a value  $V_b$  at  $r=b$ .

Equations (1) through (3) have been solved for beams having relativistic<sup>12</sup> and nonrelativistic<sup>13</sup> speeds  $v$ . The results cannot be expressed in closed analytic form in terms of elementary functions, and have therefore been given in terms of series expansions,<sup>13</sup> interpolation formulas<sup>12</sup> and computer generated outputs.<sup>12</sup> The results can be exhibited conveniently as a plot of beam current  $I$  versus the normalized potential  $V_b/V_0$ , considered as a parameter of the problem (Note that  $|V_0 - V_b|$  is just the difference between the cathode potential and the potential at the beam center  $r=0$ ). Figure 3 shows such a plot for  $eV_0/m_0c^2=3$ , for different ratios  $b/a$ . It is seen that if, for a given  $b/a$ , an attempt is made to increase the current in the beam, the potential in the center approaches closer and closer to the cathode potential. At the maximum beam current this potential difference is almost zero, and finally the intense radial space charge blocks the current entirely. Note, however, that once the maximum possible current has been exceeded (for a given  $b/a$ ) our steady-state model most likely fails; that is, the regime where the curves bend over and are steeply downward directed is no longer valid. Indeed, there is experimental evidence<sup>14</sup> that in this region the beam is unstable. However, the section of the curve lying between  $V_b/V_0=0$  and  $(V_b/V_0)_{\max}$  (corresponding to maximum current), represents stable beam propagation, and it can be traversed by gradually increasing the current while holding the accelerating voltage  $V_0$  constant. It is also observed that the larger the value of  $b/a$  the smaller

is the maximum attainable current. The reason is that with increasing  $b/a$ , the electrons must create larger radial electric fields thus reducing their speed.

The radial electric field is zero at  $r=0$  and it reaches its maximum value at the beam edge  $r=a$ , where it can be calculated from Eq. (3), once the potential  $V_a$  at the beam edge has been determined. The potential  $V_a$  is given (to second order of an iteration procedure) by Eq. (10) of Ref. 12. The sought-after electric field at the edge of the beam then takes the form,

$$- \left( \frac{aE_{\perp}}{V_0} \right) = 2 \left( \frac{m_0 c^2}{eV_0} \right) \left( \frac{I}{I_A} \right) \left( \frac{\gamma_e^{\beta_e} \gamma_c^{\beta_c}}{\gamma_e - \gamma_c} \right) \quad (r=a) \quad (4)$$

where  $I$  and  $V_0$  are the beam current and acceleration potential, respectively,

$$\gamma_e = \frac{\gamma_0 + 2\gamma_c \ln(b/a)}{1 + 2\ln(b/a)} \quad ; \quad \beta_e = (\gamma_e^2 - 1)^{1/2} / \gamma_e$$

$$\gamma_c = \left( 1 + \frac{eV_0}{m_0 c^2} \right) \left( 1 - \frac{V_b}{V_0} \right) \quad ; \quad \beta_c = (\gamma_c^2 - 1)^{1/2} / \gamma_c$$

$$\gamma_0 = [1 + (eV_0/m_0 c^2)] \quad ; \quad I_A = 4\pi\epsilon_0 m_0 c^3 / e = 17kA$$

The parameter  $V_b/V_0$  is a function of  $I$  and is found from Fig. 3. Given  $I$ ,  $V_0$  and  $(b/a)$ , the normalized electric field  $(aE_{\perp}/V_0)$  is uniquely specified. Varying  $b$  with distance  $z$  along the drift tube axis varies  $E_{\perp}$ , and formula (4) provides the basis for computing the amplitude of the spatial modulation.

For purposes of computation we assume that the electron beam fills the inner dimension of the drift tube such that  $a=b_1$  of Fig. 2. We also assume that the system is operated at maximum (i.e. limiting) current corresponding to the larger radius section,  $b_2$ .



Use of Fig. 3 and Eq. (4) then allows one to compute  $(aE_{\perp 1}/V_0)$  for the smaller sized section  $b_1$  and  $(aE_{\perp 2}/V_0)$  for the larger sized section  $b_2$ . The peak-to-peak electric field modulation of the pump is given by the difference  $a[E_{\perp 1}-E_{\perp 2}]/V_0$ . This is plotted in Fig. 4a as a function of the depth of the drift tube convolutions,  $b_2/b_1$ , together with the corresponding beam current  $I$ . The amplitude of the modulation is seen to exhibit a maximum when  $b_2/b_1=1.5$ . The appearance of the maximum is due to two competing effects. On the one hand the modulation becomes smaller and smaller as  $b_2/b_1$  approaches unity and disappears altogether when  $b_2/b_1=1$ . On the other hand, the smaller the value of  $b_2/b_1$  the larger is the limiting current (see Fig. 3) and the larger the absolute value of the electric field.

When the beam energy is increased, relativity "stiffens" the electron motion,  $v$  approaches ever closer to  $c$  and the space charge density variations decrease. Thus with increasing  $V_0$ , the fractional electric field modulation  $a[E_{\perp 1}-E_{\perp 2}]/V_0$  falls as is shown in Fig. 4b, where computations are given for the case  $eV_0/m_0c^2=9$ . Note, however, that the absolute modulation amplitude  $a(E_{\perp 1}-E_{\perp 2})$  still rises, though not dramatically, simply because  $I$  increases as  $V_0$  increases. In Fig. 5 the modulation amplitude is plotted as a function of  $V_0$ , suggesting an onset of saturation at large  $V_0$ .

Take, for example, the following experimental arrangement. A solid, unneutralized electron beam is produced by a 1.5MeV, 20kA diode and propagates through a rippled drift tube having the following dimensions:  $a=b_1=0.5\text{cm}$ ;  $b_2=0.75\text{cm}$ . We find from Fig. 4 that the peak-to-peak electric field modulation is 336 kV/cm. The ripple periodicity  $\ell$ , the spatial growth rate  $\Gamma$ , the radiated power at saturation  $P$ , and the scattering efficiency<sup>7</sup>  $\eta$  are calculated

from theory and the results are given in Table II, for two wavelengths of the stimulated, back-scattered radiation,  $\lambda=500\mu$  and  $\lambda=2\text{mm}$ .

For a longitudinal magnetic field  $B_0 \leq 8\text{kG}$  experiments conducted at both ripple periodicities given operate in the so-called high gain collective regime,<sup>7</sup> in which both scattered waves are normal modes of the plasma. Theory predicts<sup>6</sup> that cyclotron resonance effects will enhance the growth rates given in the Table by a factor of  $[1 - (e/2\pi\beta\gamma m_0 c^2) B_0 \ell]^{-1}$  as  $B_0$  is increased. For  $B_0 > 8\text{kG}$ , the  $\lambda=2\text{mm}$  interaction may enter the high gain noncollective regime<sup>7</sup> in which the growth rate exhibits a different parametric dependence on the pump electric field. To date, no experiments have been carried out in this regime.

We note that in an actual experiment, a gently curved wall ripple may be preferred, rather than the rectangular modulation shown in Fig. 2; this will reduce the chance of arcing. Also, a sinusoidal-like modulation contains fewer high frequency spatial harmonics. Alternately, a helical wall perturbation may well be contemplated, in analogy with the helical magnetic pump used previously.<sup>1, 2</sup>

### III. THE LONGITUDINAL ELECTRIC PUMP

Now we take up the problem of a relativistic electron beam subjected to a static longitudinal electric field modulation as illustrated in the lower part of Fig. 1. There is no conversion into electromagnetic radiation as was the case under discussion in Section II. In the frame of reference of the beam, the pump wave stimulates the growth of two space charge waves (plasmons). One

of these is a growing forward scattered wave, and the other a backward scattered wave. The latter is doubly Doppler upshifted in frequency and is the source of submillimeter wavelength plasmons.

The growth rate of the instability is calculated in the cold plasma approximation using fluid equations. The beam is assumed to be of infinite cross-sectional area thus reducing the problem to one dimension, which is the z axis along which the beam propagates. In the beam frame of reference in which the computations are performed (i.e. the prime frame), the relevant equations are the particle and momentum conservation equations and Poisson's equation, respectively:

$$\frac{\partial n'}{\partial t'} + N' \frac{\partial v'}{\partial z'} = - \frac{\partial}{\partial z'} (n' v') \quad (5)$$

$$\frac{\partial v'}{\partial t'} - \frac{q}{m} E' = - v' \frac{\partial}{\partial z'} (v') \quad (6)$$

$$\frac{\partial E'}{\partial z'} = \frac{q}{\epsilon_0} n' \quad (7)$$

Here  $n'$  is the perturbed rf density,  $N'$  is the average density,  $v'$  is the perturbed rf velocity;  $q$  and  $m$  are the charge and mass respectively, and  $E'$  is the z-directed rf electric field. For convenience, all nonlinear terms have been relegated to the right-hand sides of the equations. Eliminating the rf density  $n'$  from these equations yields the nonlinear wave equation for the electric field

$$\frac{\partial^2 E'}{\partial t'^2} + \omega_p'^2 E' = - \frac{\partial}{\partial t'} \left( v' \frac{\partial E'}{\partial z'} \right) + \frac{q N'}{\epsilon_0} \left( v' \frac{\partial v'}{\partial z'} \right) \quad (8)$$

which is to be solved simultaneously with Eq. (6). [ $\omega_p' = (N'e^2/m\epsilon_0)^{1/2}$  is the plasma frequency.] To this purpose we write  $E'$  and  $v'$  as

the sum of three terms corresponding to the three interacting waves:

$$E' = \frac{1}{2} \sum_{m=1,2,3} A_m(t') e^{j\psi_m} + A_m^*(t') e^{-j\psi_m} \quad (9)$$

$$v' = \frac{1}{2} \sum_{m=1,2,3} B_m(t') e^{j\psi_m} + B_m^*(t') e^{-j\psi_m}$$

where  $A_m$  and  $B_m$  are complex amplitudes that vary slowly with time, and where  $\psi_m$  is the phase given by

$$\psi_m = \omega_m t' \pm k'_m z' \quad (m=1,2,3). \quad (10)$$

(The sign in front of  $k'_m$  determines the propagation direction of the wave in question).

To solve<sup>15</sup> Eqs. (6) and (8), we substitute Eqs. (9) in, say, Eq. (8). We equate terms on the left-hand side of Eq. (6) that are periodic in  $\psi_1$  to terms on the right-hand side that have the same period  $\psi_1 = \psi_2 + \psi_3$ ; and similarly for  $\psi_2$  and  $\psi_3$ . By proceeding in this way we are invoking exact phase matching and this is synonymous to the requirement that the selection rules

$$\begin{aligned} \omega_1' &= \omega_2' + \omega_3' \\ \vec{k}_1' &= \vec{k}_2' + \vec{k}_3' \end{aligned} \quad (11)$$

be obeyed. The remaining terms that do not obey Eqs. (11) are "nonresonant" and they do not contribute to the three-wave interaction process considered. Under the assumption of a constant amplitude pump wave (wave 1) the aforementioned manipulations result in two coupled equations for the amplitude growth rates of the forward and backward scattered waves (waves 2 and 3):

$$\begin{aligned}\frac{\partial A_2}{\partial t'} &= (3/4) (k_1'/\omega_1') (q/m) A_1 A_3^*(t') \\ \frac{\partial A_3}{\partial t'} &= (3/4) (k_1'/\omega_1') (q/m) A_1 A_2^*(t')\end{aligned}\tag{12}$$

Thus, the two waves grow exponentially with a temporal growth rate given by

$$\begin{aligned}\Gamma_{t'} &= (3/4) (k_1'/\omega_1') (q/m) E'_{O||} \\ &= (3/4) (q/m) (E'_{O||}/v)\end{aligned}\tag{13}$$

where  $E'_{O||}$  is the amplitude of the pump wave. The second form of the equation comes from the fact that for the static pump wave,  $\omega_1' = vk_1'$ , with  $v$  as the beam velocity. In the cold plasma approximation, the oscillation frequency of both waves equals the plasma frequency  $\omega_p'$ , and on the basis of Eq. (11) it follows that

$$\omega_1' = 2\omega_p'\tag{14}$$

which specifies the frequency of the pump (note that the pump frequency  $\omega'$  and the wavenumber  $k' = \omega'/v$  do not represent a normal mode of the plasma). Transforming<sup>16</sup> from the beam frame to the laboratory frame, and then transforming the temporal growth rate to a spatial growth rate, leads to the formulas listed in the lower half of Table I.

In these calculations electron temperature and finite transverse beam geometry are neglected. Consequently  $k_2'$  and  $k_3'$  of the two scattered waves can take on any values as long as the momentum conservation Eq. (11),  $k_1' = k_2' - k_3'$  is satisfied. In a more realistic model, introduction of temperature eliminates the arbitrariness in  $k_1'$  and  $k_2'$ , and Landau damping further limits their values to  $k_1' L_D' \leq 1$ ,  $k_2' L_D' \leq 1$  ( $L_D'$  is the Debye length). A finite beam cross-

section and the proximity of the conducting drift tube also eliminate the arbitrariness in  $k_1'$  and  $k_2'$ . In this case the proper description of the space charge waves on the beam is given by the Trivelpiece-Gould dispersion relations.<sup>17</sup>

One way to generate a static periodic electric field  $E_{0||}$  is by charging with alternate polarity a set of equally spaced metal discs separated from one another by insulating spacers. Though viable, this method is difficult in practice considering the fact that  $E_{0||}$  needs to be several hundred kilovolts per cm. A more promising approach is once again to ripple the wall on the drift tube. Since rippling induces a density modulation, longitudinal space charge fields are created. Crude estimates suggest that the strength of this modulation can be made comparable with that shown in Figs. 4 and 5 for transverse modulation.

#### IV. DISCUSSION

The notion of rippling the wall of a drift tube or charging alternately a system of spaced discs for purposes of wave amplification (or particles acceleration) is by no means new. Here we wish to discuss the similarities and differences of the various works and compare them with the present proposals.

Nation,<sup>18</sup> Kovalev, et al<sup>19</sup> and Carmel, et al<sup>20</sup> performed experiments in which intense, relativistic electron beams were allowed to pass through corrugated metal drift tube structures. Intense microwave emission in the centimeter wavelength range was reported. In these studies the experimenters exploited the fact that a corrugated periodic waveguide can support a family of "slow" electromagnetic modes<sup>21</sup> whose phase velocity is less than  $c$ . By

adjusting the beam velocity to come into approximate phase synchronism with the electromagnetic wave, energy is extracted from the particles and the wave grows. This is a two-wave interaction process involving the slow space charge wave on the beam and a backward electromagnetic mode of the corrugated structure. The process is quite unlike the one discussed in Section II which is a three-wave interaction between the space-charge beam wave and two fast, forward electromagnetic waves. Indeed, by making our waveguide of sufficiently small diameter, we hope to cut off the lower frequency backward electromagnetic modes which participated in the interactions described in Refs. 18, 19, and 20.

Birdsall<sup>22</sup> reports the operation of the so-called "Rippled Wall Amplifier" in which a nonrelativistic beam (voltage  $\sim 700V$ , current  $\sim 10mA$ ) passes through a corrugated drift tube like that illustrated in Fig. 2. A wave launched at the input end emerges amplified at the output end. The periodicity  $\ell$  is arranged so that  $\ell = \pi v / \omega_p$ . The interaction is basically a parametric (i.e. three-wave) process in which the pump frequency is twice the plasma frequency. The interaction is very similar to that described in Section III (cf Eq. (14) and Table I) and differs in one respect only: since the beam is nonrelativistic ( $\gamma \rightarrow 1$ ), there is virtually no Doppler shift and the frequency of the growing waves is low and is given by  $\omega \approx \pi v / \ell$  [cf Table I].

In the experiments of Decker and Hirshfield<sup>23</sup> a tenuous, non-relativistic electron beam (density  $\sim 3 \times 10^5 \text{cm}^{-3}$ , voltage  $\sim 10V$ ) was subjected to quasi-static (10-300MHz) periodic electric field  $E_0$  produced by exciting a set of spaced, insulated, metal discs with a signal from an rf generator. Because of the tenuous nature of

the beam, the Debye length  $L_D' \equiv v_{th}'/\omega_p'$  was comparable with the wavelength  $\lambda'$  of the density modulation, and the pump wave interacted "resonantly" with individual electrons within their velocity distribution.<sup>24</sup> For that reason a Vlasov description of the interaction was mandatory, and the latter falls into the category of Compton-like<sup>24</sup> processes. This is unlike the collective mechanism proposed in Section III where the pump wave interacts with the velocity distribution of the dense electron beam as a whole ( $L_D' \ll \lambda'$ ) and where a fluid-mechanical description suffices (at least to lowest order).

Smith and Purcell<sup>25</sup> passed a tenuous relativistic electron beam close to the surface of an optical diffraction grating and produced light. The wavelength of the light depended on the angle of emission and on the energy of the electron beam. In this mechanism the electrons travel in near synchronism with one of the slow surface harmonic waves (phase velocity  $< c$ ) associated with the grating periodicity, and interact strongly with the longitudinal electric field component of the wave. The device is essentially a traveling wave amplifier for light, and is quite unlike the three-wave parametric systems described in this paper.

In conclusion, we have shown that the space charge of an intense, unneutralized relativistic electron beam can furnish an intense quasi-static electric pump for stimulated three-wave scattering experiments. When the electric field is transverse to the beam, the process is stimulated Raman scattering leading to emission of submillimeter electromagnetic radiation. When the electric field modulation is parallel to the beam, the three-wave process yields submillimeter wavelength plasma oscillations (plasmons). The latter could be converted to photons by one of several



processes. On the other hand, the short wavelength plasmons may be used in plasma heating experiments in which the modulated beam is injected into an ionized gas.

Wave studies with rippled drift tubes are about to begin.<sup>26</sup> The electron beam is generated by a 1.5MeV, 20kA, 30nsec accelerator (Physics International Pulserad 110A) and is confined by a ~10kG axial magnetic field. A 60cm long section of drift tube is rippled and has parameters like those given in Table II. The observations will be compared with theoretical predictions.

REFERENCES

1. L. R. Elias, W. M. Fairbank, J.M.J. Madey, H. A. Schwettman, and T. I. Smith, Phys. Rev. Lett. 36, 717 (1976).
2. D.A.G. Deacon, L. R. Elias, J.M.J. Madey, G. J. Ramian, H. A. Schwettman, and T. I. Smith, Phys. Rev. Lett. 38, 892 (1977).
3. V. L. Granatstein, S. P. Schlesinger, M. Herndon, R. K. Parker, and J. A. Pasour, Appl. Phys. Lett. 30, 384 (1977); R. K. Parker, W. M. Black, R. Tobin, M. Herndon, and V. L. Granatstein, Bull. Am. Phys. Soc. 23, 863 (1978); Y. W. Chan, Phys. Rev. Lett., 42, 92 (1979).
4. T. C. Marshall, S. Talmage, and P. Efthimion, Appl. Phys. Lett., 31, 320 (1977); also R. M. Gildenbach, T. C. Marshall, and S. P. Schlesinger, Phys. Fluids (to be published); R. M. Gildenbach, Ph.D. Thesis, 1978, Columbia University.
5. D. B. McDermott, T. C. Marshall, S. P. Schlesinger, R. K. Parker, and V.L.Granatstein, Phys. Rev. Lett. 41 1368 (1978).
6. P.Sprangle and V. L. Granatstein, Appl. Phys.Lett. 25, 377 (1974); P. Sprangle, V. L. Granatstein, and L. Baker, Phy. Rev. A12, 1697, (1975); P. Sprangle and A. T. Drobot, Naval Research Laboratory Report 3587 (1978).
7. P. Sprangle, R. A. Smith, and V. L. Granatstein, Naval Research Laboratory Report No. 3911 (1978).
8. N. M. Kroll and W. A. McMullin, Phys. Rev. A17, 300 (1978).
9. H. Motz, J. Appl. Phys. 22, 527 (1951).
10. V. P. Sukhatme and P. W. Wolff, J. Appl. Phys. 44, 2331 (1973); IEEE J. Quatum Electron, QE-10, 870 (1974).

11. J.M.J. Madey, J. Appl. Phys. 42, 1906 (1971); J.M.J. Madey, H. A. Schwettmann, and W. M. Fairbank, IEEE Trans. Nucl. Sci. 20, 980 (1973).
12. J. R. Thompson and M. L. Sloan, Phys. Fluids 21, 2032 (1978).
13. L. P. Smith and P. L. Hartman, J. Appl. Phys. 11, 220 (1940).
14. L. Smullin (private communication).
15. E. A. Frieman, J. Math. Phys. 4, 410 (1963); Physica 31, 693 (1965).
16. A. Hasegawa and K. Mima, Appl. Phys. Lett. 29, 542 (1976).
17. A. W. Trivelpiece and R. W. Gould, J. Appl. Phys. 30, 1784 (1959).
18. J. A. Nation, Appl. Phys. Lett. 17, 491 (1970).
19. N. Kovalev, M. I. Petelin, M. D. Raizer, A. V. Smorgenskii, and L. E. Tsopp, Pis'ma Zh. Eksp. Teor. Fiz. 18, 232 (1973) [JETP Lett 18, 138 (1973)].
20. Y. Carmel, J. Ivers, R. E. Kribel, and J. A. Nation, Phys. Rev. Lett. 33, 1278 (1974).
21. W. J. Kleen, Electronics of Microwave Tubes (Academic Press 1958) Chap. 18.
22. C. K. Birdsall, Proc. I.R.E. 42, 1628 (1954).
23. J. F. Decker and J. L. Hirshfield, Phys. Fluids 11, 372 (1968).
24. V. L. Granatstein and P. Sprangle, IEEE Trans. Microwave Th. and Techniques MTT25, 545 (1977).
25. S. J. Smith and E. M. Purcell, Phys. Rev. 92, 1069 (1953); J. M. Wachtel, J. Appl. Phys. 50, 49 (1979).

26. R. E. Shefer and G. Bekefi, Proceedings, IEEE International Conference on Plasma Science, Montreal P.Q., Canada, June 1979.

Table I. Stimulated scattering by relativistic electron beams in quasi-static transverse and longitudinal electric fields. All quantities are given in the laboratory frame of reference ( $\beta=v/c$ ;  $\gamma_0^2=1-\beta^2$ );  $\omega_p^2=Ne^2/m_0\epsilon_0$ .

Pump Wave	Spatial periodicity of pump $\lambda$ (m)	Frequency of back-scattered wave $\omega$ (rad. sec <sup>-1</sup> )	Spatial growth rate $\Gamma$ (m <sup>-1</sup> )
Transverse Electric Field, $E_{\perp}$	$\lambda < 2\pi\beta c\gamma_0^{3/2}/\omega_p$	$\omega = 2\pi\beta c\gamma_0^2(1+\beta)/\lambda$	$\Gamma_{\perp} = \left[ \frac{1/2 \omega_p \lambda}{8\pi\beta c} \right]^{1/2} \frac{E_{0\perp}}{m \gamma_0^2}$
Longitudinal Electric Field, $E_{\parallel}$	$\lambda = \pi\beta c\gamma_0^{3/2}/\omega_p$	$\omega = \pi\beta c\gamma_0^2/\lambda$	$\Gamma_{\parallel} = \frac{3}{4} \frac{e}{m} \frac{E_{0\parallel}}{\gamma_0^2 \beta^2}$

Table II. Parameters for a free-electron Raman laser for a peak-to-peak pump modulation of 336kV/cm and  $a=b_1=0.5\text{cm}$ ,  $b_2/b_1=1.5$ ;  $\ell$  is the pump periodicity,  $\Gamma$  the spatial growth rate,  $P$  the power at saturation, and  $\eta$  the efficiency at saturation.

	$\ell$ (cm)	$\Gamma$ ( $\text{cm}^{-1}$ )	$P$ (GW)	$\eta$ (%)
$\lambda=500$	1.3	.058	1.2	3.9
$\lambda=2\text{mm}$	3.9	.093	3.6	11.5

FIGURE CAPTIONS

- Fig. 1. Schematic drawing of static, periodic electric pump fields. In the upper figure the electric field is polarized at right angles to the direction of beam propagation. In the lower figure it is polarized along the beam direction.
- Fig. 2. Schematic drawing of a rippled drift tube.
- Fig. 3. Beam current as a function of the normalized voltage  $V_b/V_0$  for several values of  $b/a$ . The calculations were made from Eq. (20) of Ref. 12.
- Fig. 4. The normalized peak-to-peak modulation amplitude and the beam current, as a function of  $b_2/b_1$ . The electron beam fills the inner radius of the tube ( $a=b_1$ ), and the current is the limiting current for the larger-sized tube,  $b_2$ .
- Fig. 5. The maximum modulation amplitude (see Fig. 4) as a function of beam voltage, for the same conditions as those of Fig. 4.

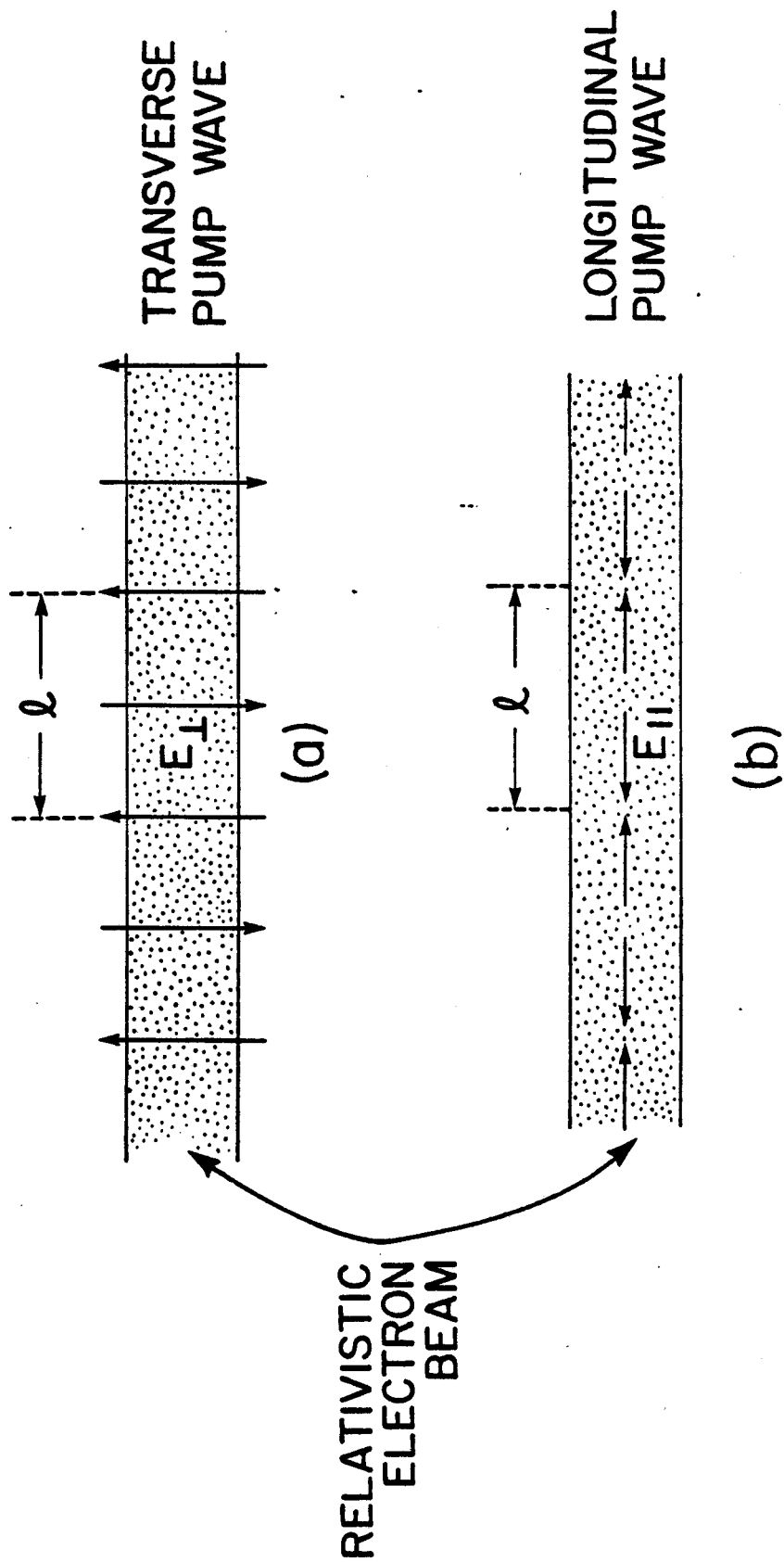


Fig. 1  
Bekefi & Shefer



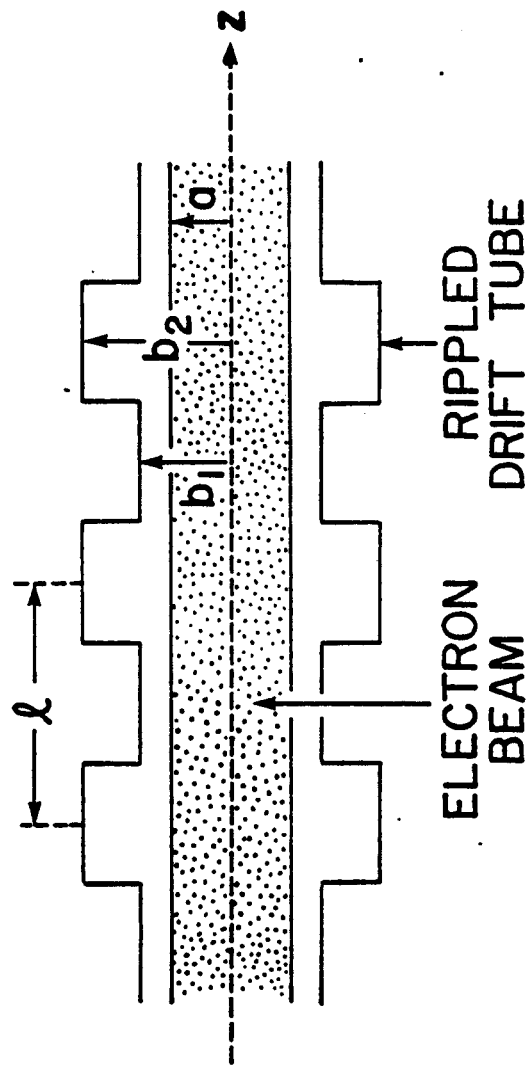


Fig. 2  
Bekefi & Shefer

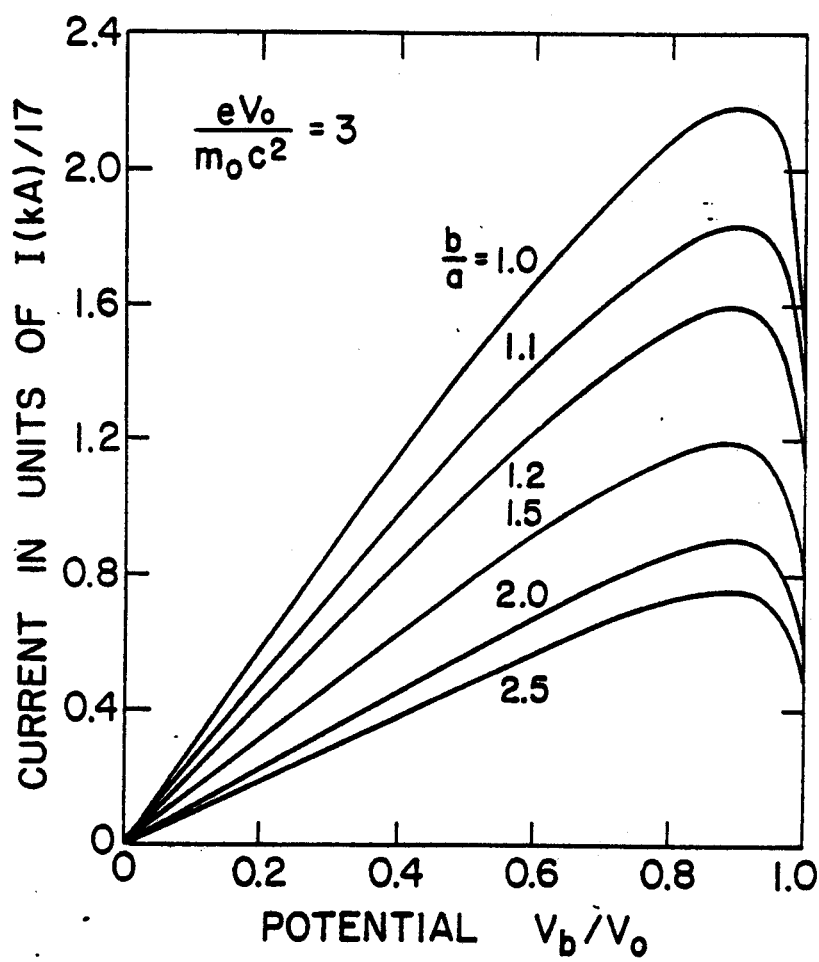
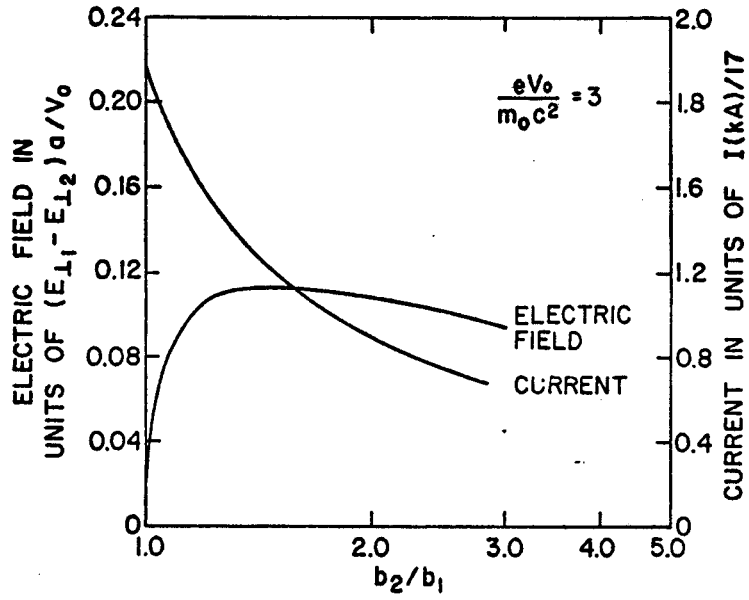
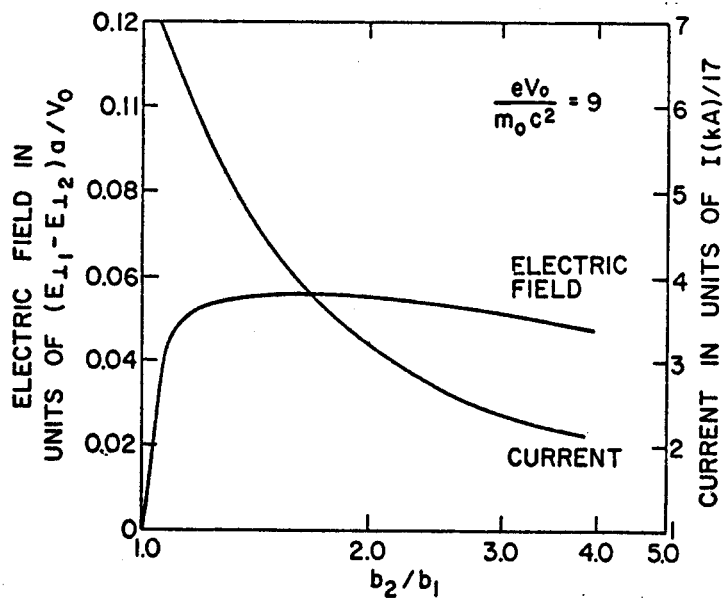


Fig. 3  
Bekefi & Shefer



(a)



(b)

Fig. 4  
Bekefi & Shefer

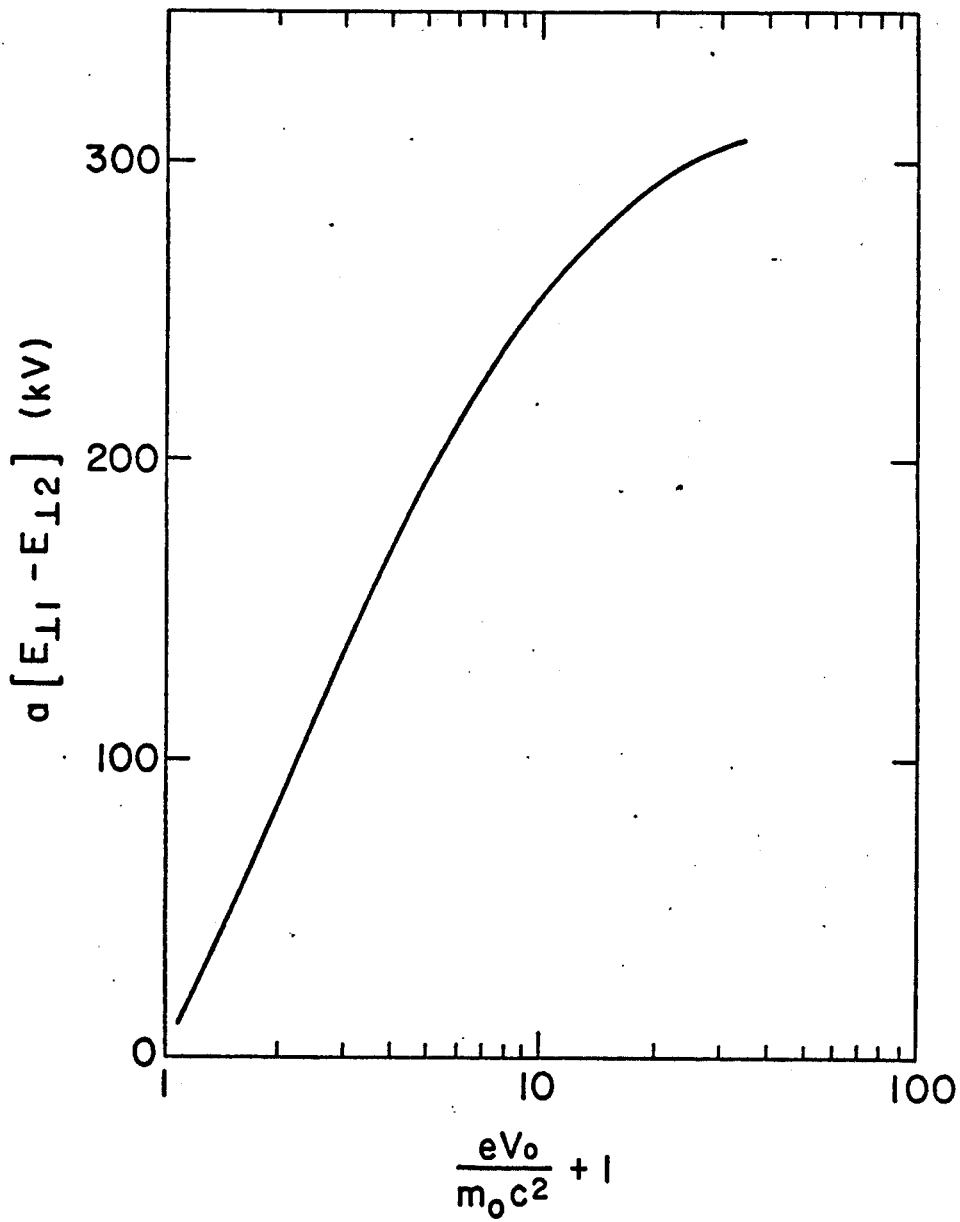


Fig. 5  
Bekefi & Shefer